Supplement of Atmos. Chem. Phys., 18, 9475–9497, 2018
https://doi.org/10.5194/acp-18-9475-2018-supplement

Atmospheric Chemistry and Physics
Open Access
EGU

Supplement of

Simulating CH_4 and CO_2 over South and East Asia using the zoomed chemistry transport model LMDz-INCA

Xin Lin et al.

Correspondence to: Xin Lin (xin.lin@lsce.ipsl.fr)

Supplementary materials

Table S1 The mean bias (±s.d.) and RMSE of the simulated annual gradient for different station groups: **(a)** CH_4 (unit: ppb), **(b)** CO_2 (ppm). Results from both ZAs and STs are presented. Statistics are given for stations outside and within the zoomed region, as well as for stations of different types within the zoomed region.

(a)

model version	statistics	outside Z	within Z	marine	mountain	coastal	continental
ST19_ED42	MB	-6.4±4.8	0.0±21.0	6.7±23.5	-3.2±10.2	-7.8±22.3	2.3±35.7
	RMSE	7.9	20.4	22.0	9.6	19.8	29.2
ZA19_ED42	MB	-0.6±8.0	3.8±16.5	15.0±18.0	-1.8±7.9	8.4±13.4	-10.4±19.3
	RMSE	7.7	16.4	22.0	7.2	13.8	18.9
ST39_ED42	MB	-6.8±4.4	0.1±22.3	7.1±24.6	-5.2±10.7	-7.3±25.5	4.9±36.6
	RMSE	8.0	21.6	23.1	10.9	22.1	30.3
ZA39_ED42	MB	-1.2±7.9	6.4±17.5	17.6±17.8	-1.9±7.8	11.9±14.5	-4.0±25.0
	RMSE	7.7	18.1	23.7	7.2	16.8	20.8

(b)

model version	statistics	outside Z	within Z	marine	mountain	coastal	continental
ST19_ED42	MB	-0.6±0.5	-0.1±2.5	-0.3±1.7	0.5±4.0	-1.5±1.8	0.2±1.9
	RMSE	0.8	2.4	1.5	3.6	2.1	1.7
ZA19_ED42	MB	-0.9±1.4	0.0±2.5	-0.3±2.2	0.2±3.9	-0.1±3.0	0.0±1.8
	RMSE	1.7	2.5	1.9	3.5	2.4	1.6
ST39_ED42	MB	-0.4±0.7	0.0±2.5	-0.1±1.7	0.5±4.0	-1.2±1.9	0.3±2.1
	RMSE	0.8	2.5	1.5	3.6	2.0	1.9
ZA39_ED42	MB	-0.9±1.4	0.1±2.6	-0.2±2.1	0.2±3.8	0.3±3.3	0.1±2.0
	RMSE	1.6	2.5	1.9	3.4	2.7	1.8

Table S2 The observed and simulated mean annual gradient of **(a)** CH_4 and **(b)** CO_2 at stations mentioned in Section 3.1.1 and Section 3.1.2. The bias reduction rates (in percentage) of ZAs compared to STs are also given for both 19-layer and 39-layer simulations.

a)

CH_4	**OBS (ppb)**	**ST19 (ppb)**	**ZA19 (ppb)**	**Bias reduction**	**ST39 (ppb)**	**ZA39 (ppb)**	**Bias reduction**
PON	32.4±12.4	2.5±11.6	31.1±7.7	95.6%	0.4±11.9	34.1±7.8	94.7%
SDZ	90.0±15.4	125.1±18.8	86.8±16.0	91.0%	128.5±19.3	100.4±22.4	73.0%
TAP	64.9±10.7	79.5±8.1	88.6±8.4	n.a.	83.9±7.5	93.3±7.8	n.a.
UUM	38.6±5.6	46.1±9.7	42.8±13.3	44.1%	49.0±11.6	49.1±8.9	n.a.

b)

CO_2	**OBS (ppm)**	**ST19 (ppm)**	**ZA19 (ppm)**	**Bias reduction**	**ST39 (ppm)**	**ZA39 (ppm)**	**Bias reduction**
PON	2.7±1.6	1.3±0.3	1.8±0.5	35.2%	1.5±0.3	1.9±0.5	37.0%
SDZ	6.8±0.5	8.8±1.3	7.7±1.9	57.9%	9.3±1.5	8.1±2.3	48.1%
TAP	6.9±1.8	7.2±0.8	10.2±0.8	n.a.	7.5±1.0	10.8±1.1	n.a.

Table S3 The correlation coefficients between the simulated and observed synoptic variability of CH_4 **(a)** and CO_2 **(b)** at PON over the period 2006–2013. The synoptic variability is calculated from residuals from the smoothed fitting curve.

(a) CH_4

Months	N. of Samples	ST19_ED42	ZA19_ED42	ST39_ED42	ZA39_ED42
Jan.–Mar.	132	0.40^{***}	0.39^{***}	0.42^{***}	0.42^{***}
Apr.–Jun.	81	0.46^{***}	0.43^{***}	0.49^{***}	0.43^{***}
Jul.–Sep.	123	0.48^{***}	0.46^{***}	0.48^{***}	0.45^{***}
Oct.–Dec.	88	0.36^{***}	0.49^{***}	0.39^{***}	0.53^{***}
All	424	0.40^{***}	0.45^{***}	0.42^{***}	0.47^{***}

(b) CO_2

Months	N. of Samples	ST19_ED42	ZA19_ED42	ST39_ED42	ZA39_ED42
Jan.–Mar.	124	-0.10	-0.24^{**}	-0.08	-0.20^{*}
Apr.–Jun.	69	-0.20	-0.23	-0.21	-0.24^{*}
Jul.–Sep.	105	-0.20^{*}	0.05	-0.22^{*}	0.02
Oct.–Dec.	83	0.05	0.08	0.02	0.06
All	381	-0.11^{*}	-0.11^{*}	-0.11^{*}	-0.11^{*}

Table S4 The statistics between the simulated and observed mean diurnal cycles of CH_4 for three exemplified stations GSN **(a)**, PON **(b)** and BKT **(c)** over specific study periods. For BKT, results from outputs extracted at a lower model level (Level=2) are presented in **(d)**. For each station, correlation coefficients and ratios of amplitudes are calculated from the simulated and observed diurnal cycles averaged over all the sampling days in a month with a complete 24-hour profile.

(a) GSN

Month	N. of Days	Amplitudes (ppb)	ST19_ED42		ZA19_ED42		ST39_ED42		ZA39_ED42	
			R	A_m/A_o	R	A_m/A_o	R	A_m/A_o	R	A_m/A_o
200801	16	13.2	0.33	0.41	0.39	1.15	0.29	0.42	0.40	1.39
200802	16	13.8	0.54^{**}	1.50	0.72^{***}	0.95	0.49^{*}	1.56	0.75^{***}	0.93
200803	24	17.6	0.48^{*}	0.11	0.51^{*}	0.66	0.50^{*}	0.14	0.45^{*}	0.75
200804	13	27.1	0.64^{**}	0.47	0.80^{***}	0.75	0.69^{***}	0.35	0.78^{***}	0.81
200805	15	28.4	-0.81^{***}	0.24	0.70^{***}	0.52	-0.86^{***}	0.18	0.63^{**}	0.43
200806	19	45.6	0.78^{***}	0.17	0.79^{***}	0.56	0.78^{***}	0.20	0.73^{***}	0.58
200807	12	24.5	-0.05	0.75	0.00	0.43	-0.11	0.85	0.32	0.44
200808	14	58.4	0.83^{***}	0.25	0.67^{***}	0.72	0.86^{***}	0.28	0.76^{***}	0.74
200809	1	63.5	0.64^{**}	0.57	0.08	0.35	0.59^{**}	0.73	0.40	0.46
200810	12	28.2	0.48^{*}	0.37	-0.29	0.85	0.47^{*}	0.45	-0.35	0.80
200811	12	19.3	-0.30	0.69	0.28	0.86	-0.52^{**}	1.08	-0.09	0.74
200812	17	17.0	0.09	0.53	0.35	0.99	0.43^{*}	0.65	0.48^{*}	1.03

* $p < 0.05$; ** $p < 0.01$; *** $p < 0.001$

(b) PON

Month	N. of Days	Amplitudes (ppb)	ST19_ED42		ZA19_ED42		ST39_ED42		ZA39_ED42	
			R	A_m/A_o	R	A_m/A_o	R	A_m/A_o	R	A_m/A_o
201108	4	187.4	0.56^{**}	0.04	0.79^{***}	0.15	0.71^{***}	0.06	0.76^{***}	0.15
201109	14	163.1	0.96^{***}	0.08	0.91^{***}	0.40	0.93^{***}	0.09	0.84^{***}	0.37
201210	25	133.5	0.87^{***}	0.13	0.96^{***}	0.50	0.83^{***}	0.18	0.95^{***}	0.68
201211	26	229.6	0.95^{***}	0.12	0.97^{***}	0.33	0.95^{***}	0.16	0.98^{***}	0.40
201212	28	206.6	0.88^{***}	0.06	0.98^{***}	0.31	0.96^{***}	0.07	1.00^{***}	0.34
201301	27	309.0	0.89^{***}	0.05	0.98^{***}	0.22	0.94^{***}	0.05	0.98^{***}	0.26
201302	20	238.9	0.79^{***}	0.08	0.97^{***}	0.27	0.85^{***}	0.08	0.97^{***}	0.32
201303	29	146.9	0.85^{***}	0.10	0.96^{***}	0.48	0.91^{***}	0.10	0.95^{***}	0.60
201304	25	121.6	0.76^{***}	0.09	0.94^{***}	0.40	0.83^{***}	0.10	0.90^{***}	0.42
201305	15	78.9	0.93^{***}	0.15	0.92^{***}	0.41	0.90^{***}	0.13	0.93^{***}	0.36

* $p < 0.05$; ** $p < 0.01$; *** $p < 0.001$

(c) BKT, at the station level

Month	N. of Days	Amplitudes (ppb)	ST19_ED42		ZA19_ED42		ST39_ED42		ZA39_ED42	
			R	A_m/A_o	R	A_m/A_o	R	A_m/A_o	R	A_m/A_o
201301	27	67.4	-0.09	0.19	0.80^{***}	0.24	-0.49^{*}	0.12	0.89^{***}	0.34
201302	17	32.5	-0.12	0.33	0.08	0.28	-0.18	0.28	0.47^{*}	0.26
201303	23	83.6	-0.22	0.14	0.70^{***}	0.21	-0.61^{**}	0.10	0.81^{***}	0.26
201304	20	47.9	-0.19	0.21	-0.05	0.21	-0.28	0.19	-0.02	0.21

201305	17	33.7	-0.60^{**}	0.31	-0.53^{**}	0.26	-0.62^{**}	0.31	-0.42^{*}	0.31
201306	18	30.6	0.18	0.92	0.17	0.51	0.03	0.84	0.43^{*}	0.51
201307	19	31.1	-0.24	0.46	-0.21	0.27	-0.37	0.47	-0.13	0.32
201308	21	50.2	-0.83^{***}	0.14	-0.42^{*}	0.13	-0.84^{***}	0.13	-0.32	0.12
201309	8	22.6	0.51^{*}	0.58	0.40	0.46	0.61^{**}	0.57	0.34	0.52
201310	16	90.8	-0.27	0.09	0.20	0.07	-0.74^{***}	0.07	0.27	0.09
201311	21	44.7	-0.11	0.24	-0.07	0.24	-0.12	0.19	-0.24	0.22
201312	22	58.3	0.50^{*}	0.17	0.87^{***}	0.34	0.57^{**}	0.11	0.80^{***}	0.43

* $p < 0.05$; ** $p < 0.01$; *** $p < 0.001$

(d) BKT, at a lower model level (Level=2)

Month	N. of Days	Amplitudes (ppb)	ST19_ED42		ZA19_ED42		ST39_ED42		ZA39_ED42	
			R	A_m/A_o	R	A_m/A_o	R	A_m/A_o	R	A_m/A_o
201301	27	67.4	0.78^{***}	0.51	0.94^{***}	0.55	0.97^{***}	0.87	0.98^{***}	0.83
201302	17	32.5	0.78^{***}	0.99	0.87^{***}	0.71	0.83^{***}	1.64	0.74^{***}	1.21
201303	23	83.6	0.86^{***}	0.38	0.91^{***}	0.50	0.89^{***}	0.67	0.84^{***}	0.67
201304	20	47.9	0.72^{***}	0.32	0.60^{**}	0.22	0.72^{***}	0.55	0.72^{***}	0.38
201305	17	33.7	0.37	0.42	0.01	0.30	0.85^{***}	0.64	0.88^{***}	0.43
201306	18	30.6	0.56^{**}	1.64	0.57^{**}	0.84	0.55^{**}	2.18	0.53^{**}	1.17
201307	19	31.1	0.72^{***}	0.73	0.46^{*}	0.30	0.82^{***}	1.13	0.70^{***}	0.56
201308	21	50.2	0.65^{**}	0.24	0.53^{**}	0.16	0.83^{***}	0.46	0.77^{***}	0.38
201309	8	22.6	0.10	0.80	0.09	0.63	-0.22	1.24	-0.13	1.26
201310	16	90.8	0.81^{***}	0.22	0.82^{***}	0.13	0.95^{***}	0.35	0.91^{***}	0.27
201311	21	44.7	0.44^{*}	0.43	0.38	0.29	0.70^{***}	0.61	0.60^{**}	0.29
201312	22	58.3	0.69^{***}	0.55	0.81^{***}	0.67	0.85^{***}	1.07	0.87^{***}	1.02

* $p < 0.05$; ** $p < 0.01$; *** $p < 0.001$

Table S5 The statistics between the simulated and observed mean diurnal cycles of CO_2 for three exemplified stations GSN **(a)**, PON **(b)** and BKT **(c)** over specific study periods. For BKT, results from outputs extracted at the surface model level (Level=1) are presented in **(d)**. For each station, correlation coefficients and ratios of amplitudes are calculated from the simulated and observed diurnal cycles averaged over all the sampling days in a month with a complete 24-hour profile.

(a) GSN

Month	N. of Days	Amplitudes (ppm)	ST19_ED42		ZA19_ED42		ST39_ED42		ZA39_ED42	
			R	A_m/A_o	R	A_m/A_o	R	A_m/A_o	R	A_m/A_o
200801	10	2.3	0.01	0.17	0.00	0.30	0.12	0.26	0.04	0.45
200802	13	4.0	0.59^{**}	0.45	0.78^{***}	0.27	0.56^{**}	0.47	0.81^{***}	0.26
200803	20	2.2	-0.52^{**}	0.22	0.70^{***}	0.49	-0.64^{**}	0.19	0.53^{**}	0.42
200804	17	3.2	0.79^{***}	0.27	0.74^{***}	0.32	0.82^{***}	0.27	0.72^{***}	0.37
200805	13	2.8	0.47^{*}	0.12	-0.36	0.14	0.33	0.03	-0.43^{*}	0.12
200806	12	3.5	-0.30	0.08	0.10	0.07	-0.42^{*}	0.11	-0.26	0.08
200807	12	4.4	0.40	0.34	0.50^{*}	0.18	0.54^{**}	0.33	0.70^{***}	0.21
200808	15	5.3	0.25	0.11	0.59^{**}	0.40	0.30	0.14	0.66^{***}	0.36
200809	9	5.8	-0.73^{***}	0.16	0.00	0.30	-0.82^{***}	0.15	-0.26	0.33
200810	13	4.0	-0.36	0.22	-0.74^{***}	0.51	-0.34	0.27	-0.74^{***}	0.52
200811	8	1.8	0.90^{***}	0.55	0.90^{***}	1.09	0.83^{***}	0.23	0.85^{***}	0.84
200812	20	1.7	-0.48^{**}	0.35	0.09	0.80	-0.50^{**}	0.35	0.25	0.65

* $p < 0.05$; ** $p < 0.01$; *** $p < 0.001$

(b) PON

Month	N. of Days	Amplitudes (ppm)	ST19_ED42		ZA19_ED42		ST39_ED42		ZA39_ED42	
			R	A_m/A_o	R	A_m/A_o	R	A_m/A_o	R	A_m/A_o
201108	4	42.4	0.36	0.01	0.43^{*}	0.03	0.41^{*}	0.02	0.28	0.03
201109	14	30.4	0.90^{***}	0.02	0.83^{***}	0.10	0.86^{***}	0.02	0.72^{***}	0.11
201210	25	23.2	0.83^{***}	0.04	0.94^{***}	0.12	0.78^{***}	0.06	0.95^{***}	0.16
201211	26	35.7	0.86^{***}	0.03	0.92^{***}	0.05	0.85^{***}	0.04	0.91^{***}	0.06
201212	28	30.1	0.60^{**}	0.01	0.96^{***}	0.04	0.77^{***}	0.01	0.95^{***}	0.05
201301	27	38.2	0.81^{***}	0.01	0.07	0.02	0.84^{***}	0.01	0.02	0.02
201302	20	36.5	0.84^{***}	0.02	0.34	0.02	0.81^{***}	0.02	0.54^{**}	0.02
201303	29	29.9	0.88^{***}	0.05	0.95^{***}	0.13	0.91^{***}	0.04	0.97^{***}	0.17
201304	25	19.4	0.77^{***}	0.10	0.94^{***}	0.35	0.80^{***}	0.11	0.92^{***}	0.37
201305	15	13.4	0.89^{***}	0.11	0.56^{**}	0.28	0.87^{***}	0.11	0.51^{*}	0.29

* $p < 0.05$; ** $p < 0.01$; *** $p < 0.001$

(c) BKT, at the station level

Month	N. of Days	Amplitudes (ppm)	ST19_ED42		ZA19_ED42		ST39_ED42		ZA39_ED42	
			R	A_m/A_o	R	A_m/A_o	R	A_m/A_o	R	A_m/A_o
201301	27	23.1	0.04	0.07	0.52^{**}	0.08	-0.07	0.05	0.52^{**}	0.11
201302	17	20.3	0.09	0.07	0.54^{**}	0.06	-0.25	0.04	0.66^{***}	0.09
201303	23	25.3	-0.08	0.06	0.46^{*}	0.08	-0.34	0.04	0.60^{**}	0.10
201304	20	22.3	-0.17	0.06	0.26	0.06	-0.42^{*}	0.04	0.48^{*}	0.07

201305	17	19.5	-0.35	0.05	0.32	0.05	-0.64^{**}	0.05	0.50^{*}	0.08
201306	18	21.3	-0.53^{**}	0.07	0.16	0.06	-0.83^{***}	0.06	0.40	0.08
201307	20	19.7	-0.09	0.07	0.60^{**}	0.06	-0.38	0.05	0.68^{***}	0.07
201308	19	22.3	0.62^{**}	0.06	0.96^{***}	0.05	0.49^{*}	0.05	0.95^{***}	0.07
201309	8	14.2	0.82^{***}	0.06	0.84^{***}	0.11	0.71^{***}	0.05	0.84^{***}	0.14
201310	16	23.8	-0.09	0.06	0.40	0.06	-0.37	0.04	0.61^{**}	0.07
201311	21	42.4	-0.29	0.03	0.11	0.03	-0.58	0.02	0.42^{*}	0.04
201312	22	27.9	0.00	0.05	0.49^{*}	0.06	-0.22	0.03	0.37	0.08

* $p < 0.05$; ** $p < 0.01$; *** $p < 0.001$

(d) BKT, at the surface model level (Level=1)

Month	N. of Days	Amplitudes (ppm)	ST19_ED42		ZA19_ED42		ST39_ED42		ZA39_ED42	
			R	A_m/A_o	R	A_m/A_o	R	A_m/A_o	R	A_m/A_o
201301	27	23.1	0.95^{***}	0.42	0.97^{***}	0.48	0.96^{***}	0.52	0.97^{***}	0.57
201302	17	20.3	0.96^{***}	0.44	0.97^{***}	0.50	0.97^{***}	0.57	0.97^{***}	0.63
201303	23	25.3	0.97^{***}	0.39	0.97^{***}	0.46	0.96^{***}	0.50	0.96^{***}	0.54
201304	20	22.3	0.93^{***}	0.40	0.96^{***}	0.42	0.95^{***}	0.51	0.96^{***}	0.52
201305	17	19.5	0.93^{***}	0.47	0.96^{***}	0.43	0.94^{***}	0.61	0.95^{***}	0.59
201306	18	21.3	0.92^{***}	0.48	0.94^{***}	0.40	0.93^{***}	0.55	0.94^{***}	0.51
201307	20	19.7	0.94^{***}	0.39	0.97^{***}	0.37	0.96^{***}	0.50	0.96^{***}	0.49
201308	19	22.3	0.92^{***}	0.17	0.95^{***}	0.25	0.90^{***}	0.25	0.94^{***}	0.33
201309	8	14.2	0.93^{***}	0.45	0.89^{***}	0.33	0.95^{***}	0.52	0.88^{***}	0.41
201310	16	23.8	0.98^{***}	0.42	0.97^{***}	0.48	0.97^{***}	0.55	0.95^{***}	0.61
201311	21	42.4	0.96^{***}	0.21	0.97^{***}	0.24	0.96^{***}	0.28	0.97^{***}	0.28
201312	22	27.9	0.86^{***}	0.36	0.90^{***}	0.42	0.91^{***}	0.45	0.92^{***}	0.52

* $p < 0.05$; ** $p < 0.01$; *** $p < 0.001$

Figure S1 (a) Map of locations of airports in South and East Asia from the Comprehensive Observation Network for TRace gases by AIrLiner (CONTRAIL) project (Machida et al., 2008). **(b)** Close-up map for airports in Japan and Republic of Korea. The whole region is divided into four subregions, namely East Asia (EAS), the Indian sub-continent (IND), Northern Southeast Asia (NSA) and Southern Southeast Asia (SSA), and all the airports and vertical profiles are grouped into the four subregions accordingly. The zoomed grid of the LMDz-INCA model is also plotted as background.

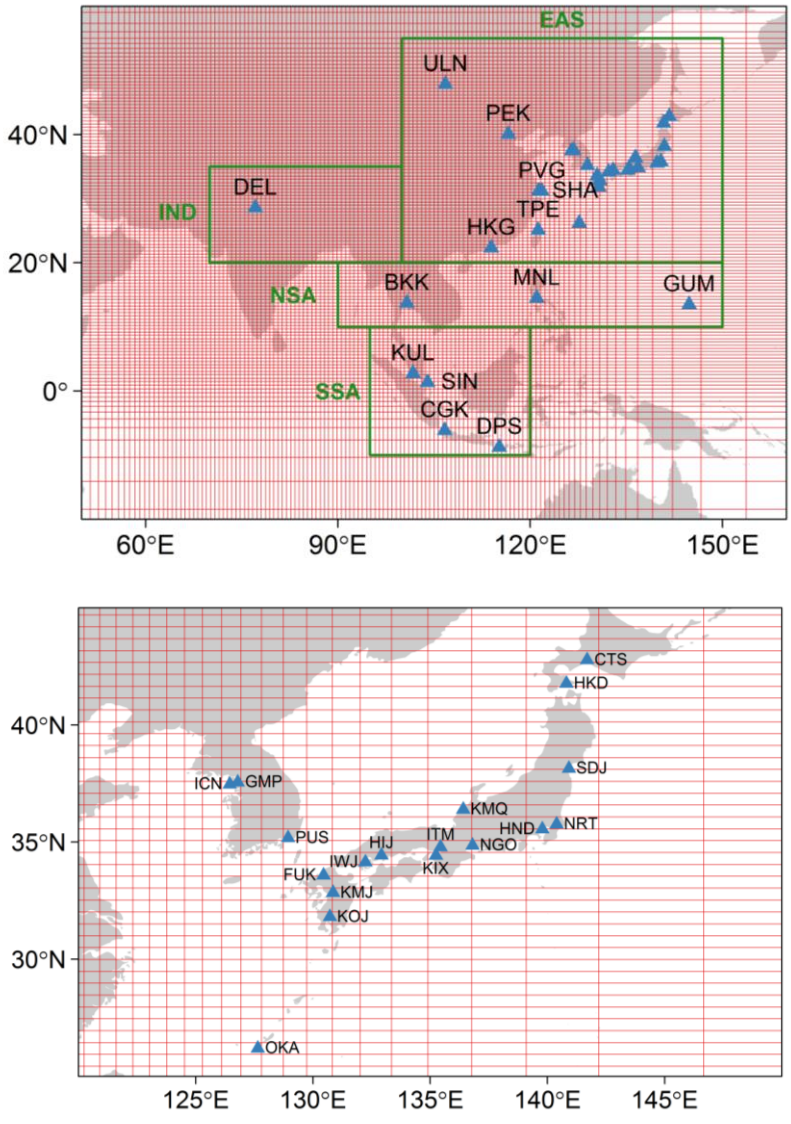

Figure S2 Sampling dates of CO_2 measurements for airports in Figure S1. For each airport, only sampling dates with vertical profiles available (i.e. measurements during ascending or descending flights) are plotted.

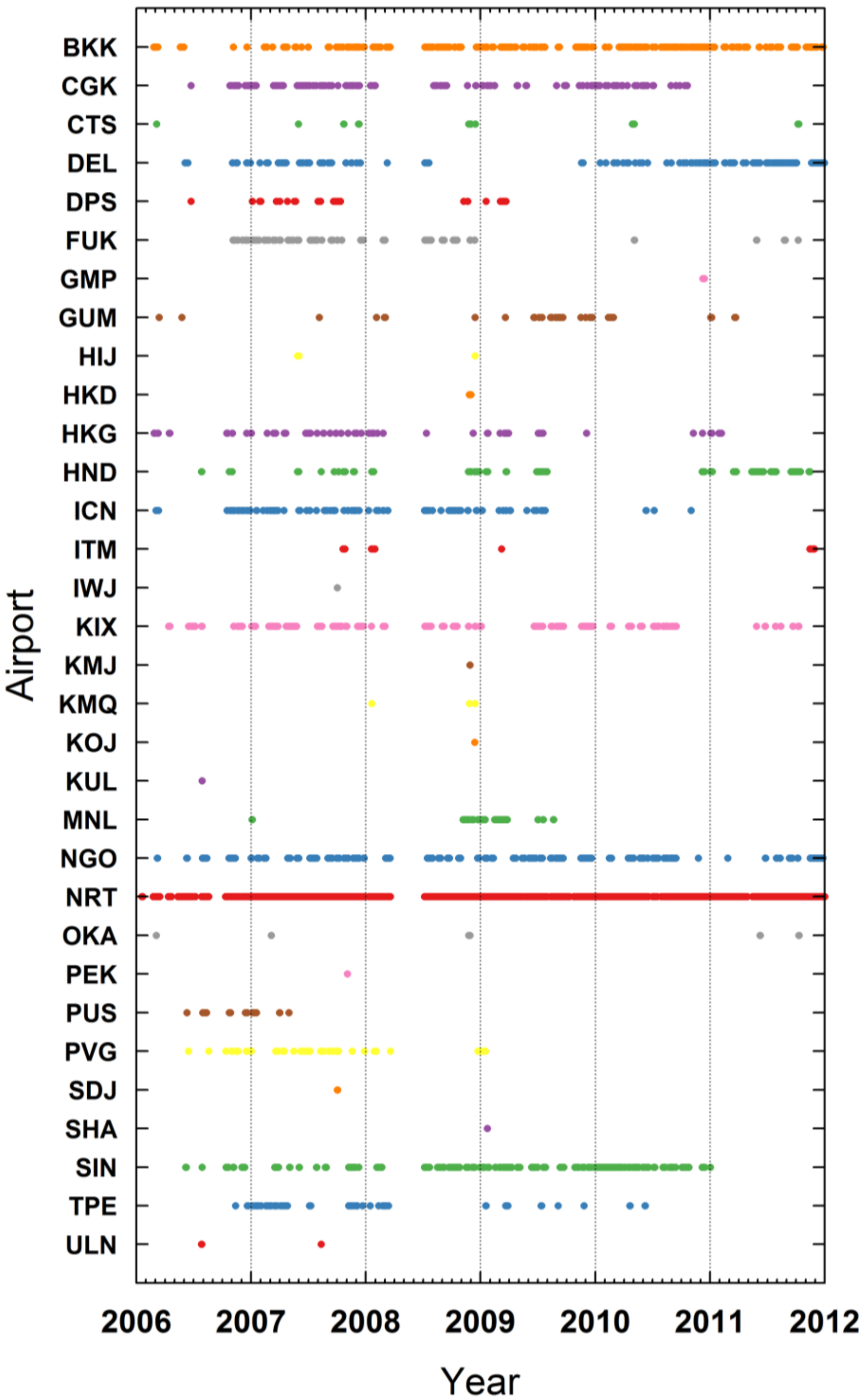

Figure S3 Scatterplots of the simulated and observed CH_4 mean annual gradients between HLE and other stations for January–March **(a)**, April–June **(b)**, July–September **(c)**, and October–December **(d)**. In each panel, the simulated CH_4 gradients are based on simulations from the standard (blue circles) and zoom (red circles) versions, respectively. The black dotted line indicates the identity line, whereas the blue and red dotted lines indicate the corresponding linear fitted lines. The closed and open circles represent stations inside and outside the zoomed region.

(a) January–March

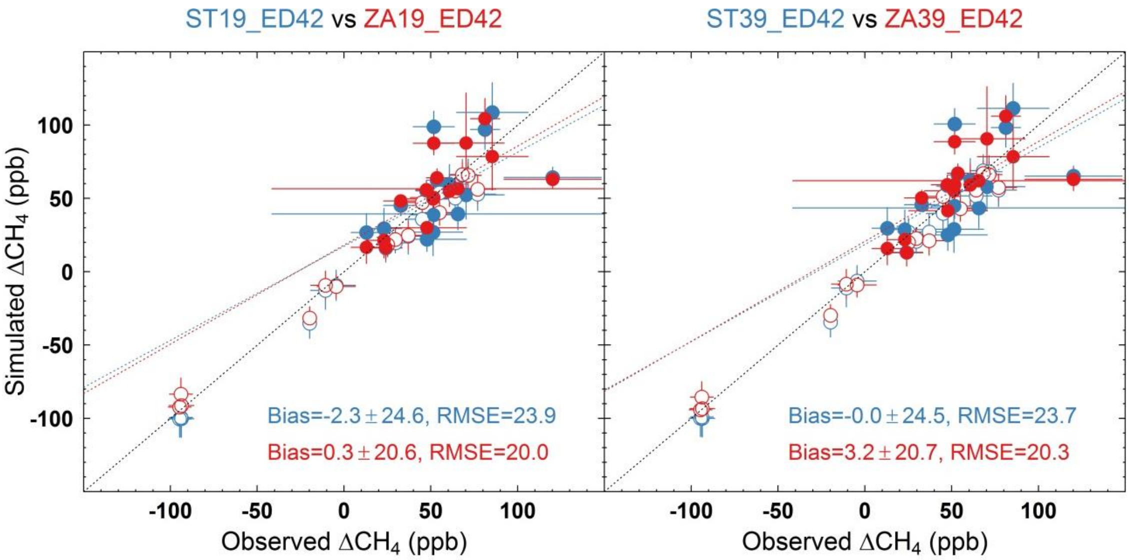

(b) April–June

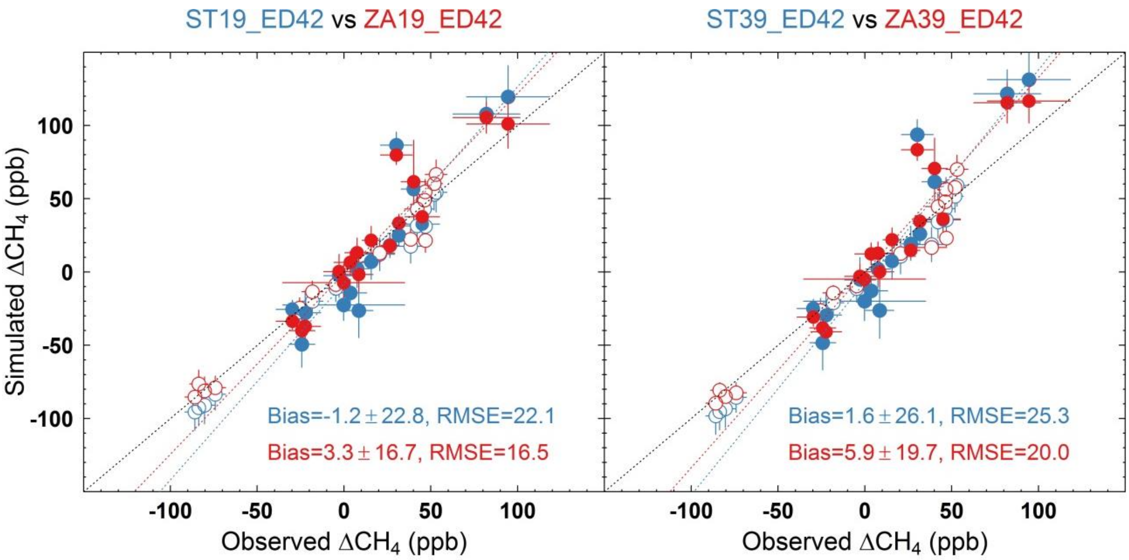

(c) July–September

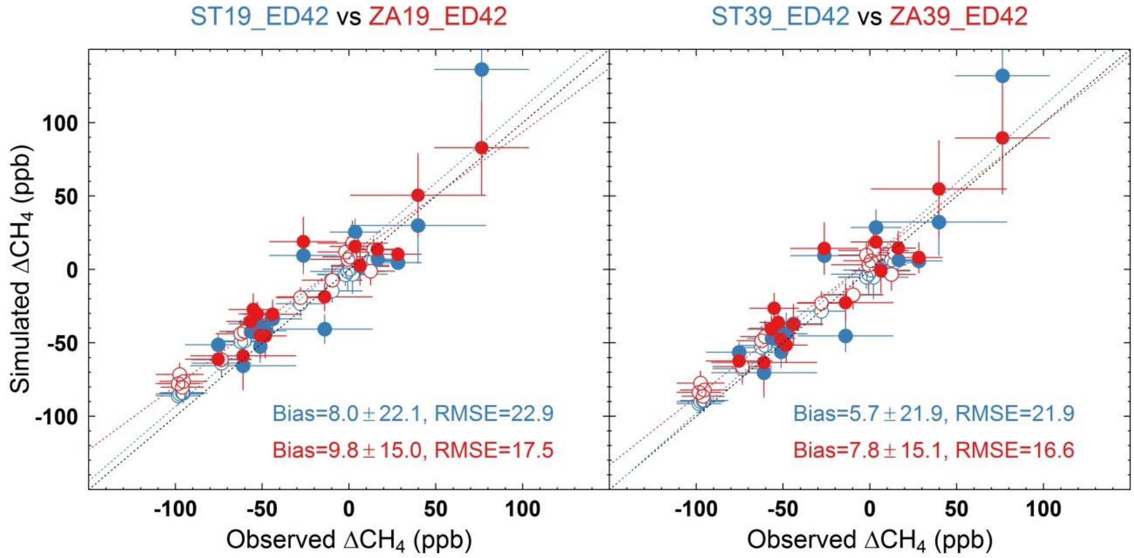

(d) October–December

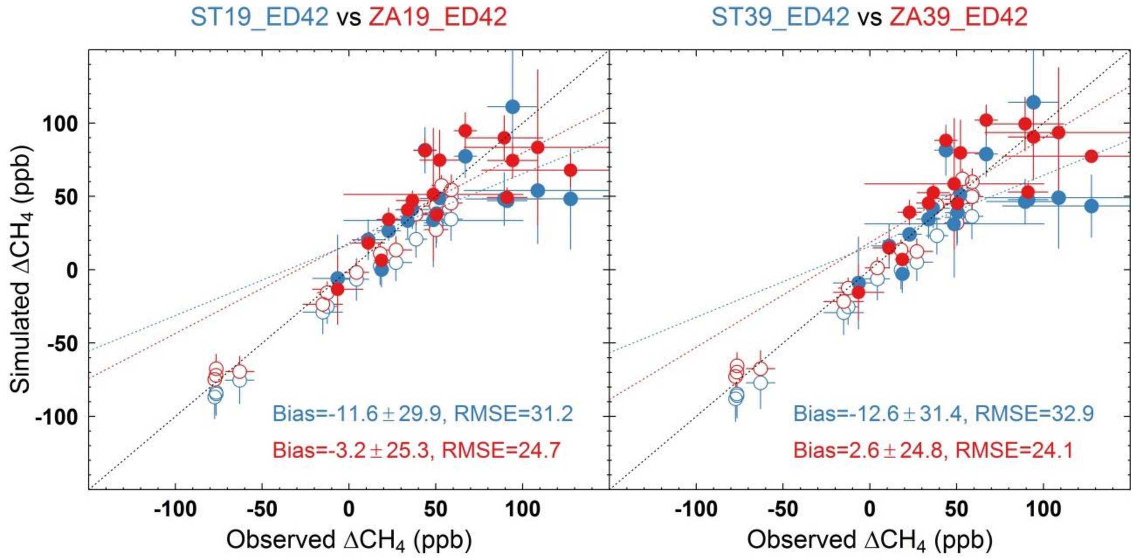

Figure S4 CH_4 surface flux maps for South and East Asia (SEA), based on two different inventories of anthropogenic emissions for the year 2010 from EDGARv4.2FT2010 and EDGARv4.3.2 (http://edgar.jrc.ec.europa.eu). CH_4 hotspots, defined as the grids with emission rates stronger than 1×10^{-9} kg CH_4 m^{-2} s^{-1} ($\approx$0.8 Tg CH_4 yr^{-1}), are indicated by blue dots. Both maps are generated in ZA grid meshes and with the same biogenic CH_4 fluxes as given in Table 1.

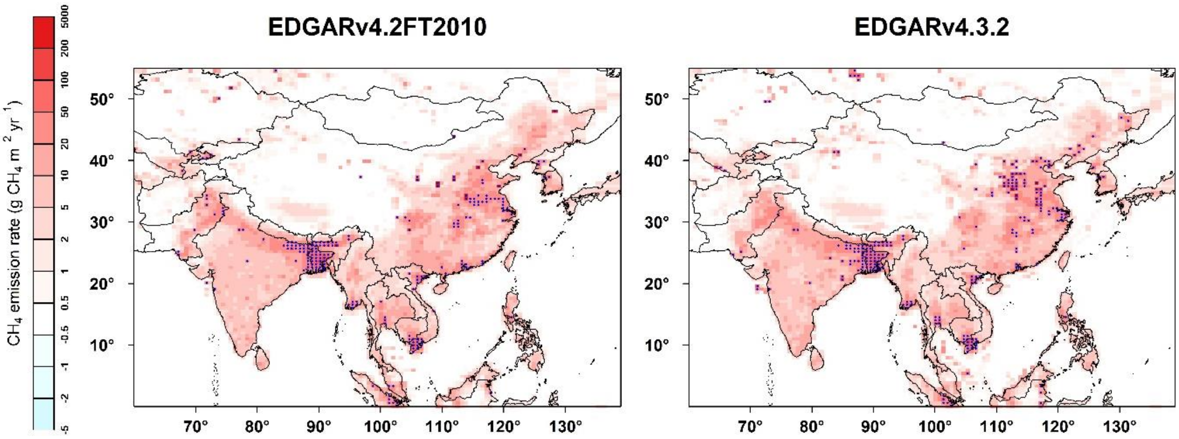

Figure S5 Maps of CH_4 surface fluxes (upper panels) and CH_4 concentration fields at the first model level (lower panels) for the year 2010. Results from both ZA and ST with 19 model layers

are presented for comparison.

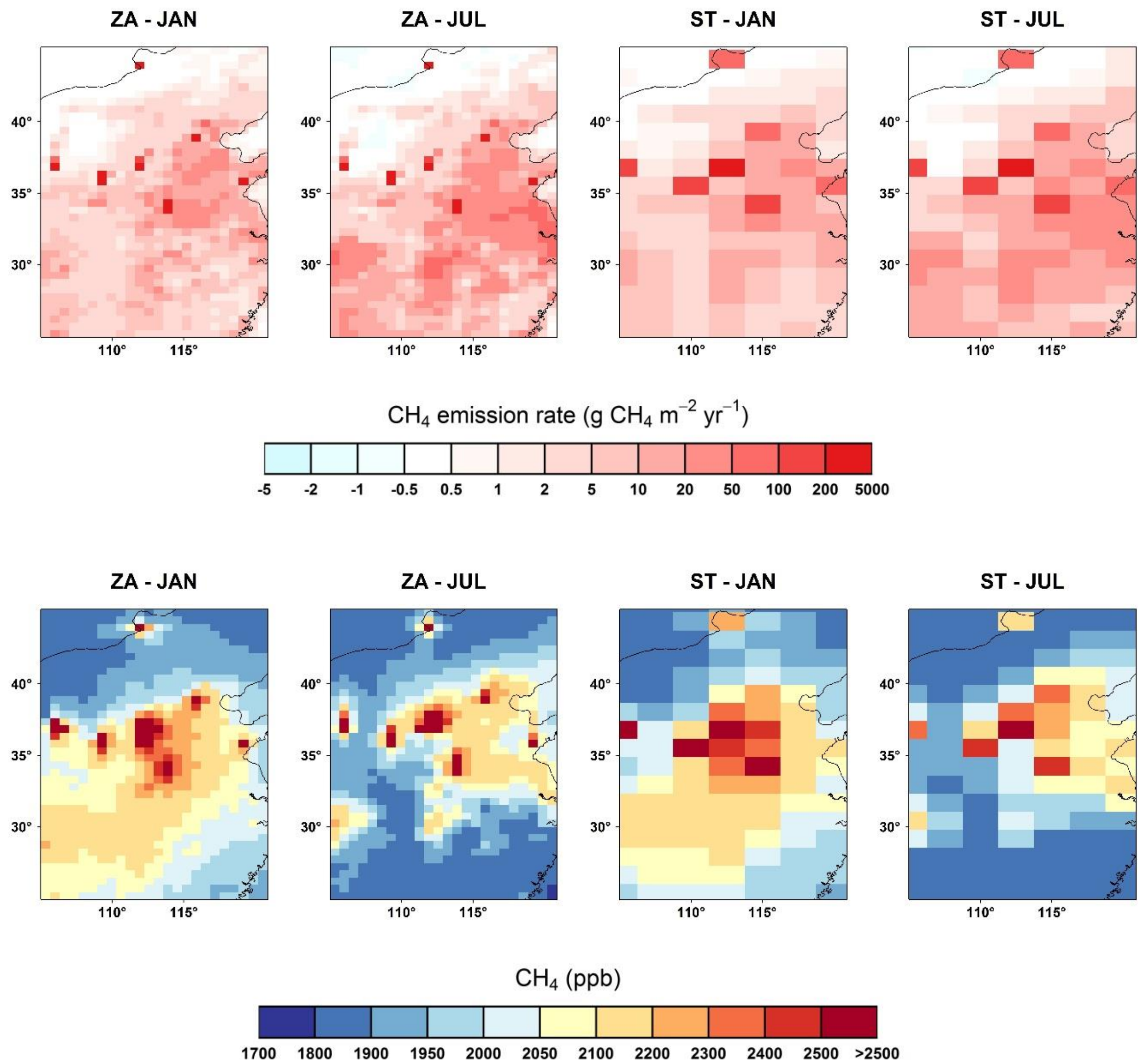

Figure S6 The spatial distributions of mean annual CH_4 fluxes around the stations SDZ, PON, CRI, GSN, TAP and UUM for the year 2010 mapped with the ZAs model grids. The black meshes indicate the STs model grids. The black dot denotes the location of the station, whereas the 3×3 meshes colored in green indicate the grid where the station is located (the 'center grid') and its 8 neighbors.

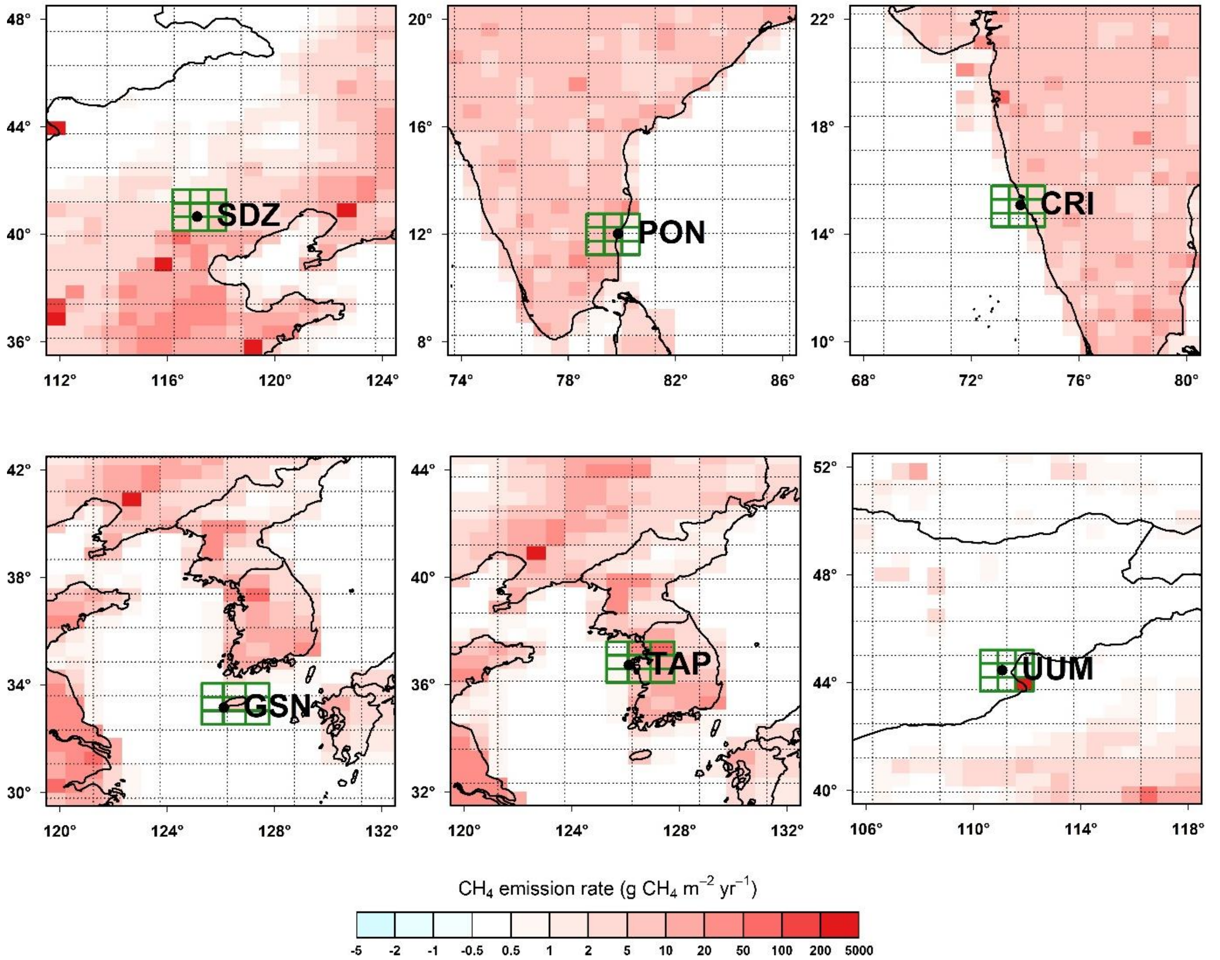

Figure S7 Scatterplots of simulated and observed CO_2 mean annual gradients between HLE and other stations for January–March **(a)**, April–June **(b)**, July–September **(c)**, and October–December **(d)**. In each panel, the simulated CO_2 gradients are based on simulations from the standard (blue circles) and zoom (red circles) versions, respectively. The black dotted line indicates the identity line, whereas the blue and red dotted lines indicate the corresponding linear fitted lines. The closed and open circles represent stations inside and outside the zoomed region.

(a) January–March

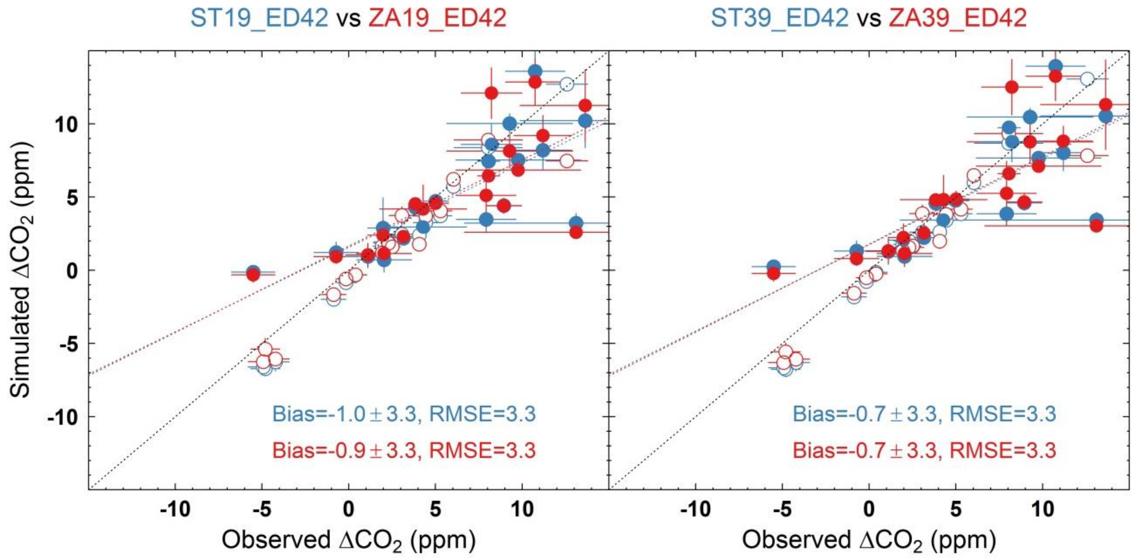

(b) April–June

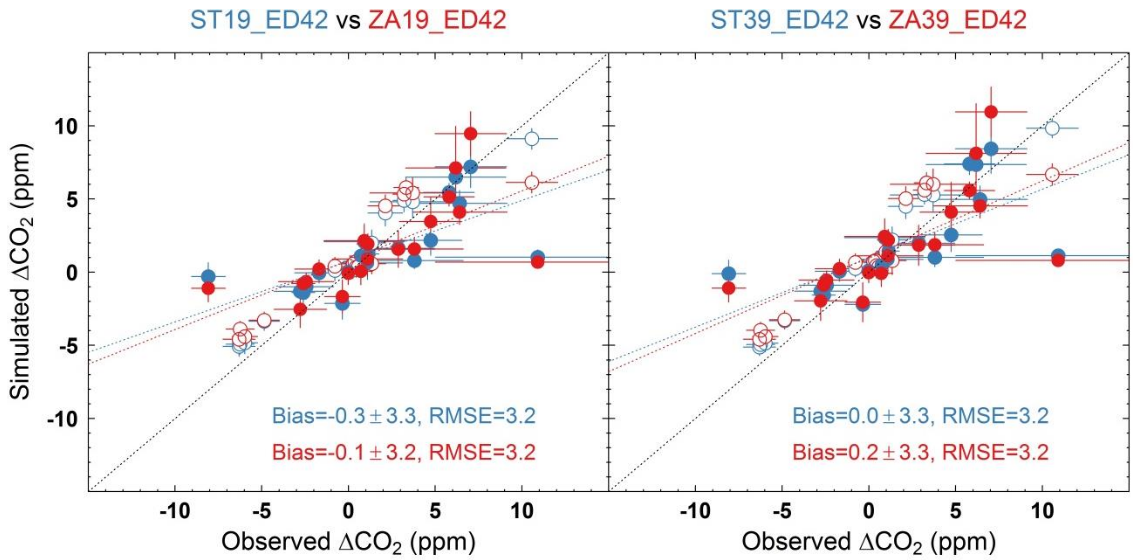

(c) July–September

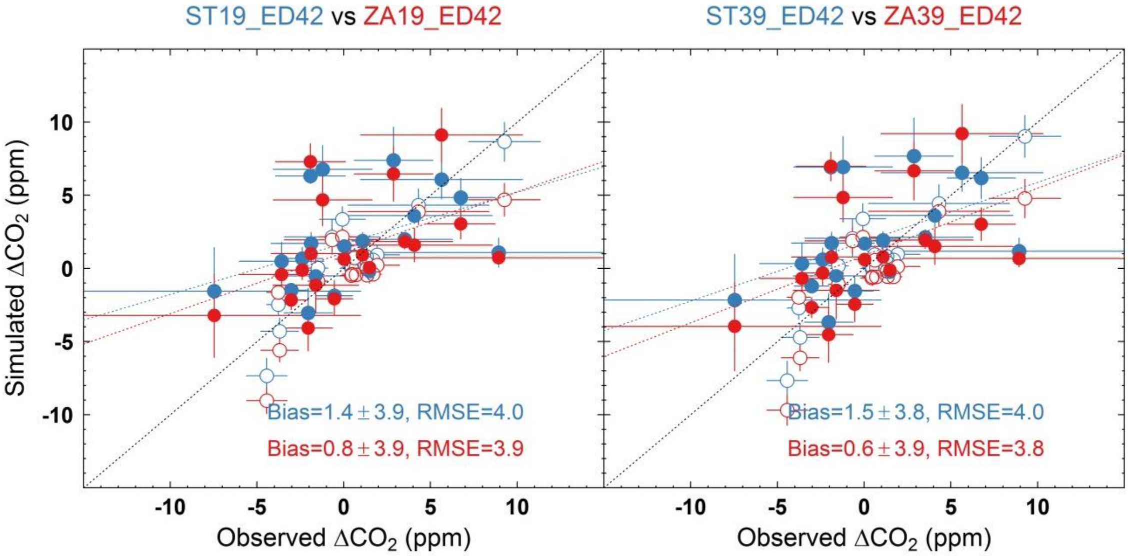

(d) October–December

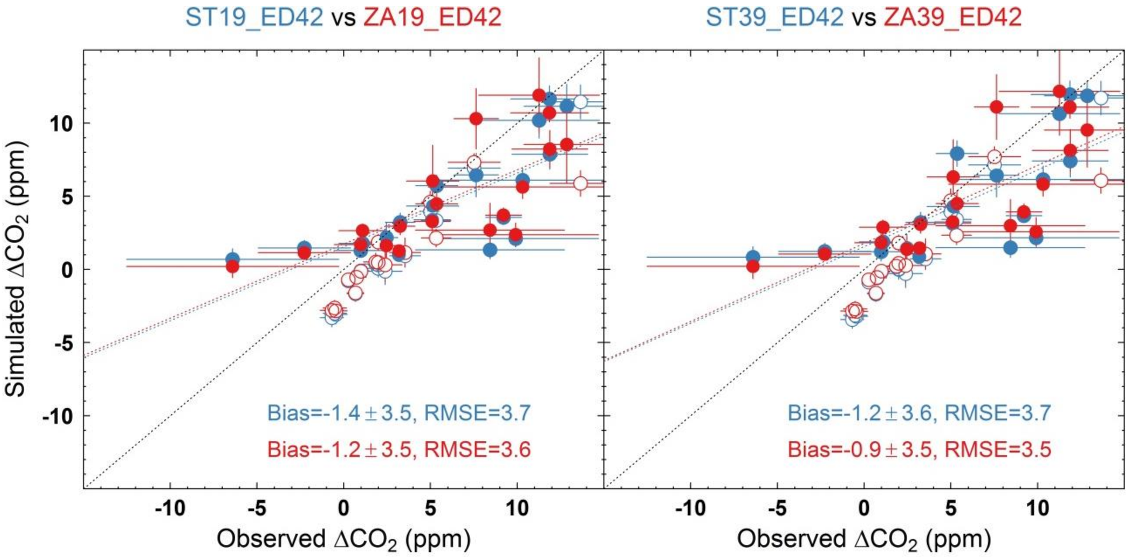

Figure S8 The spatial distributions of mean annual CO_2 fluxes around the station TAP for the year 2010 mapped with the ZAs model grids. The black meshes indicate the STs model grids. The black dot denotes the location of the station, whereas the 3×3 meshes colored in green indicate the grid where the station is located (the ‘center grid’) and its 8 neighbors.

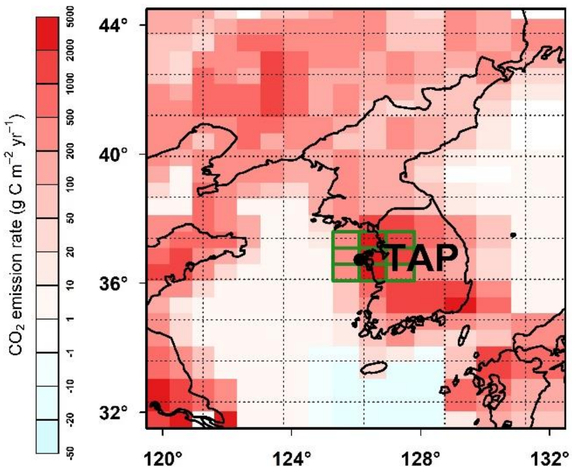

Figure S9 The observed and simulated mean seasonal cycles of CH_4 for KZM, WLG and UUM. In each panel, the colors of lines are defined as Figure 3. In addition, we also show the mean seasonal cycles from sensitivity test simulations prescribed with wetland emissions from ORCHIDEE outputs (green and orange lines for the standard and zoom versions, respectively). The text shows statistics between the simulated and observed seasonal cycles for 39-layer models.

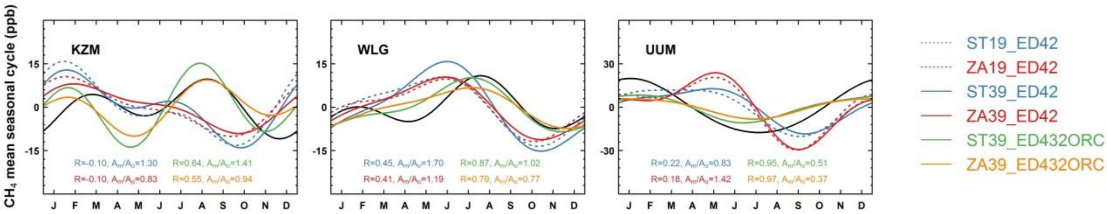

Figure S10 The observed and simulated mean seasonal cycles of CH_4 for stations outside the zoomed region. In each panel, the simulated mean seasonal cycles are based on simulations from the standard (blue lines) and zoom (red lines) versions, respectively. The text shows statistics between the simulated and observed seasonal cycles for 39-layer models.

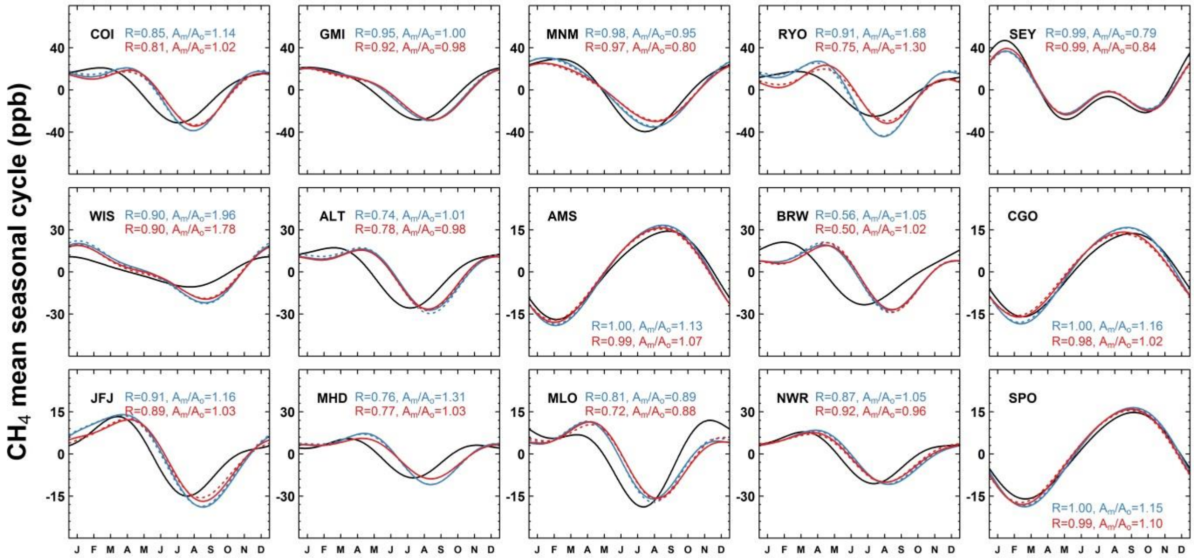

Figure S11 The observed and simulated mean seasonal cycles of CO_2 for stations outside the zoomed region. In each panel, the simulated mean seasonal cycles are based on simulations from the standard (blue lines) and zoom (red lines) versions, respectively. The text shows statistics between the simulated and observed seasonal cycles for 39-layer models.

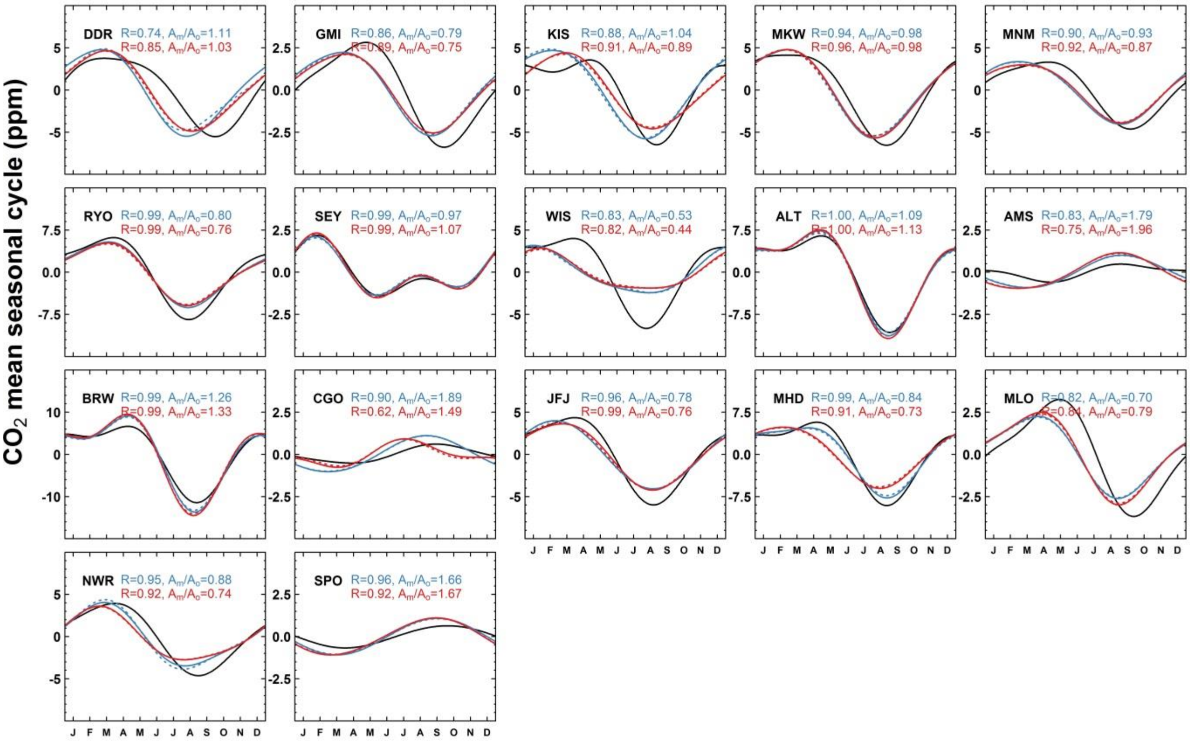

Figure S12 The correlations and normalized standard deviations between the simulated and observed synoptic variability for CH_4 **(a,b)** and CO_2 **(c,d)** at stations outside the zoomed region. For each station, the synoptic variability is calculated from residuals from the smoothed fitting curve.

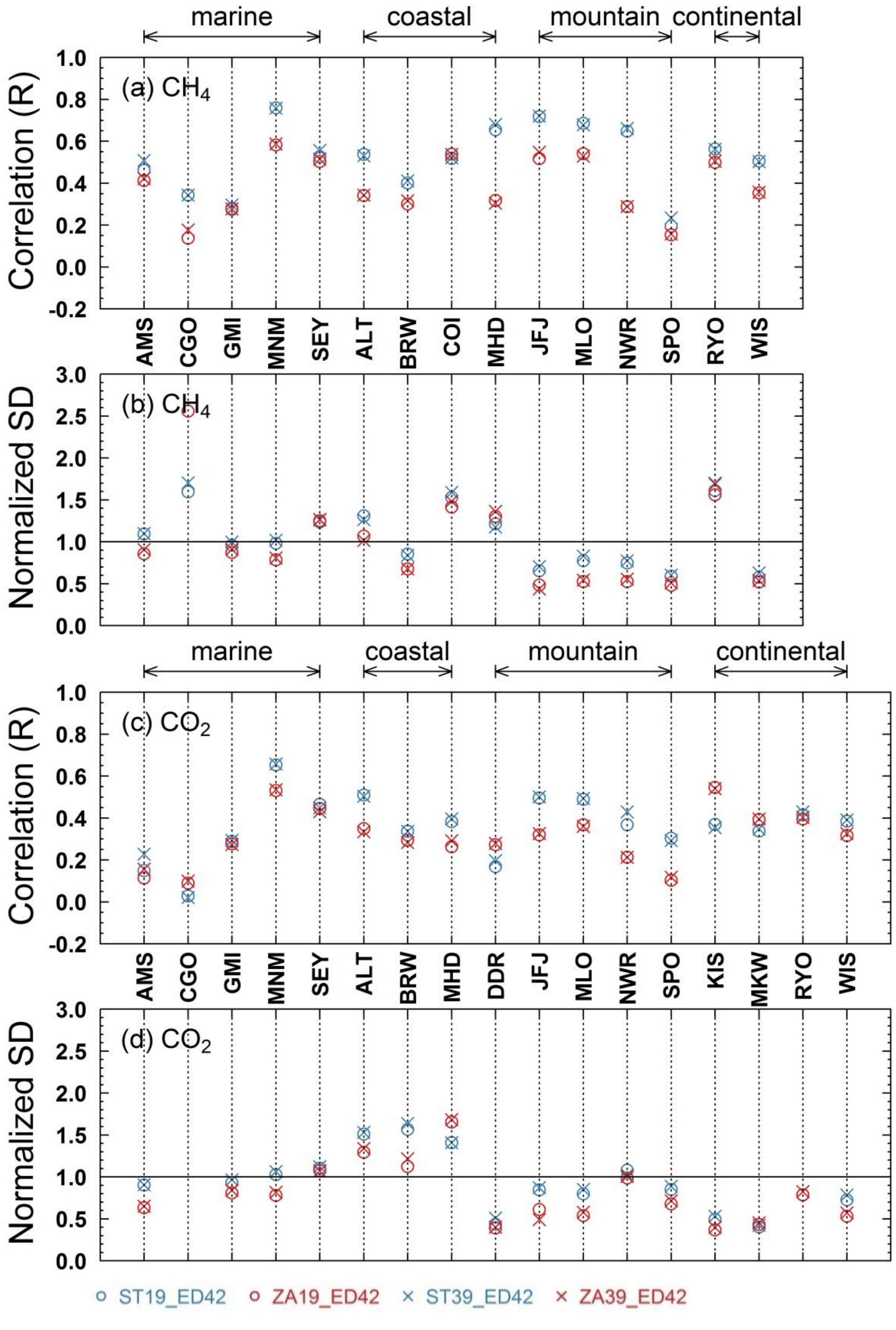

Figure S13 Time series of observed and simulated CH_4 synoptic variabilities at UUM over the period 2006–2013. The synoptic variability is calculated from residuals from the smoothed fitting curve.

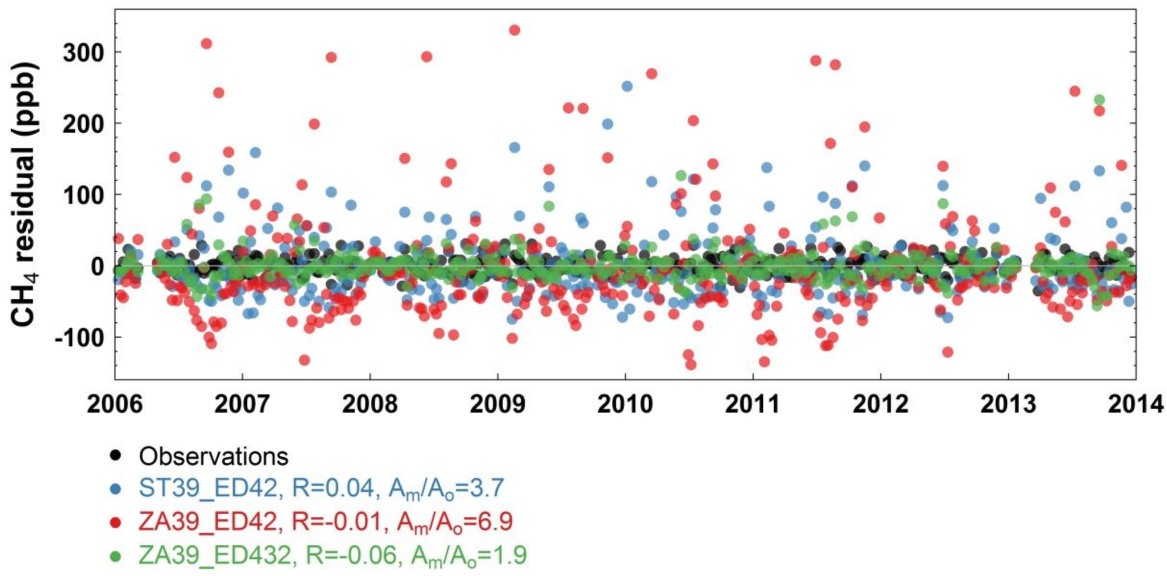

Figure S14 Time series of observed and simulated CH_4 **(a)** and CO_2 **(b)** synoptic variabilities at PON over the period 2006–2013. For each trace gas, the synoptic variability is calculated from residuals from the smoothed fitting curve.

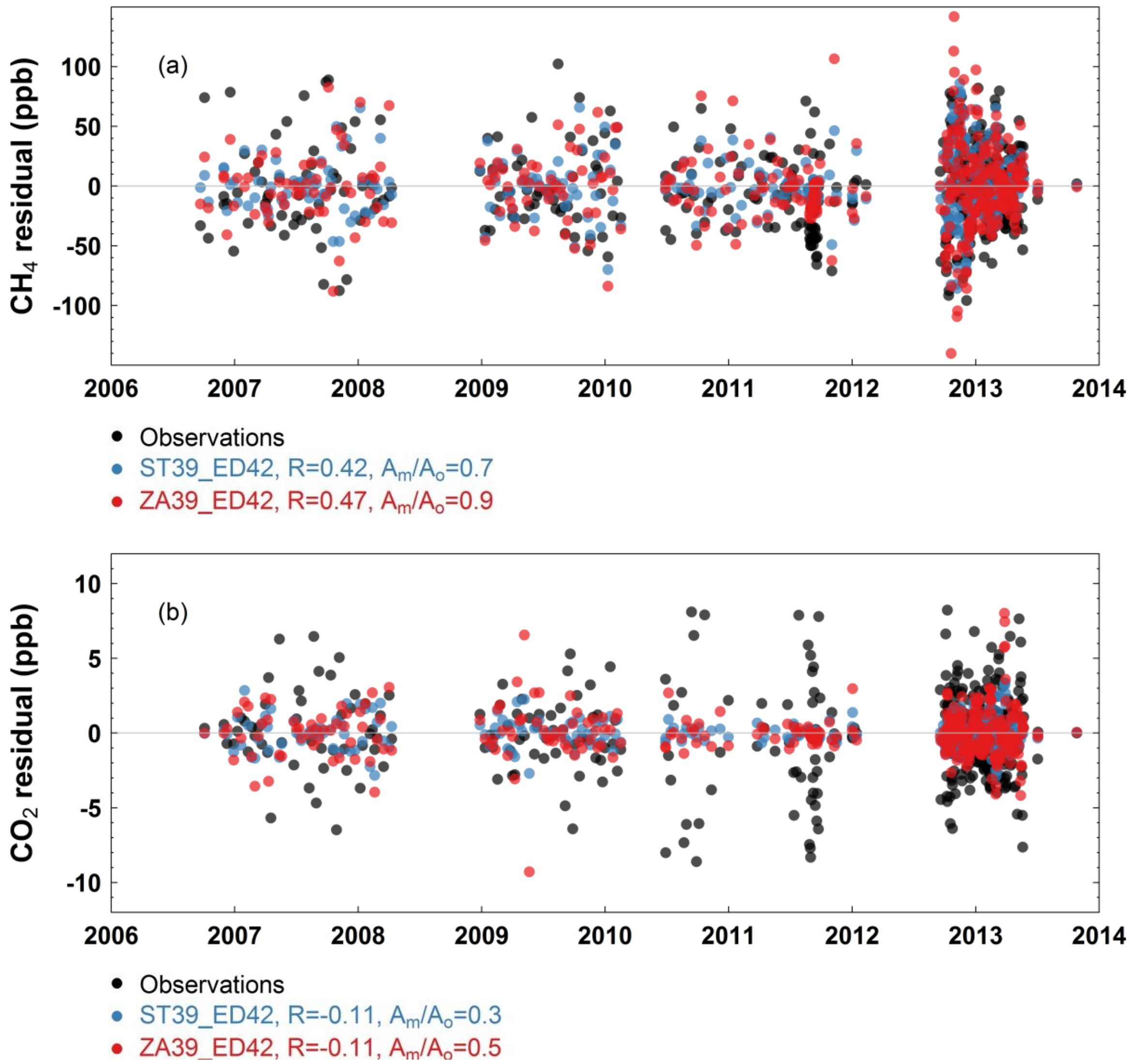

Reference

Machida, T., Matsueda, H., Sawa, Y., Nakagawa, Y., Hirotani, K., Kondo, N., Goto, K., Nakazawa, T., Ishikawa, K. and Ogawa, T.: Worldwide Measurements of Atmospheric CO_2 and Other Trace Gas Species Using Commercial Airlines, J. Atmos. Ocean. Technol., 25(10), 1744–1754, doi:10.1175/2008JTECHA1082.1, 2008.